

Progress toward full optical control of ultracold-molecule formation: Role of scattering Feshbach resonances

Roland Lefebvre and Osman Atabek ^{*}

Université Paris-Saclay, CNRS, Institut des Sciences Moléculaires d'Orsay, 91405 Orsay, France



(Received 10 February 2020; accepted 19 May 2020; published 15 June 2020)

Feshbach resonances play a major role in translationally cold-molecule preparation. In this context, their laser control is of crucial importance. This work is devoted to the depiction of some basic mechanisms of such a control using intense, short laser pulses and referring to nonlinear multiphoton processes. Our goal is to adiabatically transport a Feshbach resonance onto a zero-width resonance, the characteristics of which have already been discussed in the literature. Three processes are then addressed: (i) during the rise of the pulse and its plateau, the preparation of a so-called laser bound molecule (LBM) still stable, but structurally different from the standard chemically bound molecule; (ii) during the pulse switching off, an adiabatic transport of this LBM on a very few excited vibrational levels, and (iii) concomitantly, a filtration strategy to photodissociate all these levels except one, giving thus rise to but a single field-free excited vibrational state. With or without an eventual stimulated Raman adiabatic passage technique to bring all the population to the ground rovibrational state, this opens an alternate for a full optical control of ultracold-molecule formation. The illustrative example, offering the potentiality to be transposed to other diatomics, is H_2^+ .

DOI: [10.1103/PhysRevA.101.063406](https://doi.org/10.1103/PhysRevA.101.063406)

I. INTRODUCTION

Feshbach resonances (FR) are widely referred to when preparing ultracold molecules [1]. The most common approach deals with FRs as scattering resonances resulting from a bound state of the diatomic molecule embedded in the collisional continuum describing the translational motion between the pair of free atoms. Molecules can be produced near a FR, and an adiabatic sweep of the electromagnetic field driving the dynamics can be used as an efficient method for converting ultracold (i.e., low translational energy) atoms into ultracold molecules [2,3]. The efficiency of the method is expected to be importantly increased if the FR lifetime is controlled by some external fields. Moreover, it remains that translationally cold molecules prepared by this method are vibrationally excited. The overall story line for ultracold-molecule preparation we are proposing can be sketched as a laser control addressing three objectives: (i) During the rise of the optical pulse, an initial scattering wave packet describing the colliding pair of atoms has to be efficiently connected to a long-range molecular FR. (ii) For an optimal trapping, during the pulse plateau, this FR should be controlled to ensure the best possible overlap with the collisional wave packet, together with the longest possible lifetime, to avoid loss and decay mechanisms. (iii) At the end of the pulse, the FR should be connected with but a single field-free molecular vibrational level v of its ground electronic state. Thermodynamically speaking, in terms of Boltzmann distributions, even if this $v \neq 0$, the system is considered ultracold, as is explained later, using an additional laser to bring it, when necessary, to its

vibrationless state. This work is mainly devoted to the last two objectives, the first one being based on considerations already discussed in the literature. In particular, initial wave packets describing either a condensate embedded in an optical trap [4,5], or continuum states in a free condensate [6] have been referred to in collisional deactivation mechanisms, with experimental achievements on Na [2].

We have recently developed a robust laser coherent control scheme (based on a destructive interference mechanism) to substantially increase FR lifetimes by adiabatically driving them into so-called zero-width resonances (ZWR). Up to date, this has mainly been used to design a filtration strategy aiming at molecular rovibrational cooling [7–9]. This work is rather devoted to a laser optimal control scheme to energy localize and increase sharpness, and consequently efficiency of FRs that mediate the scattering dynamics itself. In the ultracold-molecule context, two types of Feshbach resonances have been referred to: (i) A single electronic state in field-free conditions leading to a so-called light-assisted self-induced Feshbach resonance [5]. The corresponding wave function is peaked at short internuclear distances (close to the diatomic equilibrium geometry) leading to a situation deviating from universality and opening the way to ultracold chemistry. We have recently studied such a resonance illustrated in the case of RbSr, a polar paramagnetic heteronuclear diatomic with a strong permanent dipole moment [10]. (ii) Two electronic states which are field coupled by a transition dipole moment μ leading to the standard definition. Such FRs pertain to the so-called universal decay regime [11]. Motivated by this context, this study is devoted to FRs of the second category. With the restriction to a one-dimensional, two-state model without permanent dipoles (in each electronic states) that we are adopting, all considerations on the basic control

^{*}osman.atabek@u-psud.fr

mechanisms concerning laser-induced FRs and ZWRs are directly applicable to any rotationless homonuclear diatomics. H_2^+ is but a simple illustrative example. The objective is to produce and control a FR with eigenenergy close to (i.e., slightly below) the dissociation threshold, and consequently with a wave function peaked at large internuclear distances. The physical process in consideration is a laser-assisted low-energy atomic collision close to the dissociation threshold of the ground $1s\sigma_g$ state of H_2^+ , taken as the origin of energies, a situation described in a field-dressed Floquet model with a diabatic curve crossing at rather large internuclear distances (close to the right turning point of the highest excited vibrational levels $v = 17, 18$). The energy distribution (bandwidth) of the collisional wave packet is assumed broad enough to overlap with these ground-state excited vibrational levels, but more importantly with the vibrational level $v_+ = 0$ accommodated by the upper adiabatic potential $V_+(R)$ originating from $1s\sigma_g$ and the single-photon-dressed $2p\sigma_u$ excited states. In other words, the closer the laser controlled $v_+ = 0$ to the dissociation limit and sharper could be chosen the energy distribution. This adiabatic vibrational level has to be further considered as initiating the Feshbach resonance, with an expected energy that could even exceed the one of the highest v 's. As a consequence, large probability density is deposited at rather large internuclear distances (here at about $R \simeq 13$ a.u. as compared to $R \simeq 2$ a.u. for the equilibrium geometry). When switching on the laser, this $v_+ = 0$ state will be considered as a Feshbach resonance, in relation with its standard Fano-type definition of a discrete vibrational level embedded in, and radiatively coupled to, the continuum of the lower adiabatic potential $V_-(R)$, through a nonadiabatic coupling. The diabatic coupling is written as $\mu\sqrt{I}$, I being the laser field intensity. Increasing the intensity will result in two modifications: (i) the level will be shifted toward higher energies bringing it in even better overlap with the collisional wave packet; and (ii) as a resonance, it will acquire a width Γ that could be controlled through the intensity. An increase of intensity will produce a linear increase of Γ , as expected in the weak-field regime. On the contrary, higher intensities pertaining to the strong-field regime can lead to a decrease of Γ , as they induce weaker nonadiabatic interactions. This refers to the well-known vibrational trapping mechanism [12–14]. The overall expected observation is that the collisional wave packet be trapped in such a Feshbach resonance with probability density at large internuclear distances. When the laser pulse is switched off, the population returns back to field-free levels $v = 17, 18$ which have the most favorable Franck-Condon (FC) overlaps. The interest is that a rather narrow (long-lived) and energy-controllable Feshbach resonance can trap, for a long enough duration, the collisional wave packet at large internuclear distance, with rather well-defined and limited spatial extension range, such that at the end of the pulse, the FC overlap favors the right turning point of a (hopefully) single vibrational level, $v = 17$ or 18 , for instance.

Our aim is to produce, playing both with the laser wavelength and intensity, a ZWR from the Feshbach resonance in consideration. If we are successful in doing this, i.e., producing $\Gamma = 0$, or less ambitiously, by substantially decreasing Γ (vibrational trapping mechanism), we will be in a situation

to control the single (or few) vibrational level(s) which is (are) expected to be ultimately prepared. In other words, the translational motion will be trapped in a long-lived FR at large distance, ensuring its cooling. This FR (or hopefully ZWR) with a short spatial extension (Gaussian-type wave function for $v_+ = 0$) will transfer the probability density to a single vibrational level ($v = 17$ or 18). If actually we succeed this single vibrational level population, the vibrational cooling is already achieved. A stimulated rapid adiabatic passage (STIRAP) process [15] could then transfer the population to the vibrationless ground state, as previously demonstrated with Sr_2 molecules [16,17]. In this work we show how to proceed for specific choices of laser wavelengths and intensities to produce ZWRs, i.e., in principle, infinitely long-lived resonances. Apart from their interest in molecular cooling, such exotic states correspond to specific molecules exhibiting different structural properties and which exist only during the laser excitation process. We call them laser bound molecules (LBM) as opposite to the usual field-free chemically bound molecules (CBM). Although our model and conclusions are worked out on the simplest, lightest, nonpolar H_2^+ molecular system, we claim their potentiality to be transposed to other systems. Actually, it is worth noting that the relative first sight simplicity of H_2^+ goes together with some numerical and model challenges in relation with the particular asymptotic form of its so-called charge resonance enhanced transition dipole [18,19]. This necessitates to reconsider the semiclassical destructive interference interpretation of the ZWR for generalizing it to a multiphoton excitation scheme that should be properly described. In turn, this brings additional confidence to the transposition argument opening the way to strong-field excitation.

The paper is organized as follows. Section II is devoted to the Floquet model and exploratory calculations for the critical determination of laser characteristics. The results for long-range FRs at a laser wavelength $\lambda = 25 \mu\text{m}$ are presented in Sec. III, with special emphasis on the role of charge resonance enhanced transition dipole, and multiphoton issues affecting FRs. The interference mechanism in play for the ZWR and the LBM versus CBM characterizations are discussed in Sec. IV, before concluding in Sec. V.

II. MODEL CONSIDERATIONS AND CRITICAL DETERMINATION OF LASER PARAMETERS

In this section, we examine the rather unexpected property of long-range localized FR, candidate for describing a so-called laser bound molecule (LBM) state, originating from a bound state which, although strongly coupled to a dissociative continuum, has the possibility to acquire an infinite (or quasi-infinite) lifetime. Such exotic resonances have already been discussed in the literature, first in the context of accidentally narrow rotational lines in predissociation [20,21], then as bound states in continuum (BIC) [22,23], and more recently as zero-width resonances (ZWR) [24]. In the following, the physical context is collisional molecular formation by photoassociation, the illustrative example being H_2^+ .

A. Floquet model and exploratory calculations

We briefly recall the model used to describe the strong-field induced photodissociation dynamics of a rotationless

laser-aligned H_2^+ molecule, with only two electronic states labeled $|g\rangle$ (for the ground $1s\sigma_g$ state) and $|u\rangle$ (for the excited $2p\sigma_u$ state) [25]. The time-dependent wave function is expanded on this electronic basis:

$$|\Phi(R, t)\rangle = |\phi_g(R, t)\rangle|g\rangle + |\phi_u(R, t)\rangle|u\rangle \quad (1)$$

with nuclear wave functions obtained from the time-dependent Schrödinger equation written in (2×2) matrix form:

$$i\hbar \frac{\partial}{\partial t} \begin{bmatrix} \phi_g(R, t) \\ \phi_u(R, t) \end{bmatrix} = \left(T_N + \begin{bmatrix} V_g(R) & 0 \\ 0 & V_u(R) \end{bmatrix} - \mu(R)\mathcal{E}(t) \begin{bmatrix} 0 & 1 \\ 1 & 0 \end{bmatrix} \right) \begin{bmatrix} \phi_g(R, t) \\ \phi_u(R, t) \end{bmatrix}. \quad (2)$$

T_N represents the nuclear kinetic energy operator. $V_g(R)$ and $V_u(R)$ are the Born-Oppenheimer (BO) potentials. $\mu(R)$ is the electronic transition dipole moment between states $|g\rangle$ and $|u\rangle$. $\mathcal{E}(t)$ is the linearly polarized electric field amplitude. For a continuous wave laser,

$$\mathcal{E}(t) = E \cos(\omega t) \quad (3)$$

with an intensity ($I \propto E^2$), a frequency ω , and a wavelength $\lambda = 2\pi c/\omega$, c being the speed of light. The Floquet ansatz for such a time-periodic Hamiltonian gives [25]

$$\begin{bmatrix} \phi_g(R, t) \\ \phi_u(R, t) \end{bmatrix} = e^{-iE_v t/\hbar} \begin{bmatrix} \chi_g(R, t) \\ \chi_u(R, t) \end{bmatrix} \quad (4)$$

with time periodic $\chi_k(R, t)$ ($k = g, u$) which can be Fourier expanded:

$$\chi_k(R, t) = \sum_{n=-\infty}^{\infty} e^{in\omega t} \varphi_k^n(R) \quad (5)$$

with unknown components satisfying a set of coupled differential equations written in compact form, for any n :

$$\begin{aligned} [T_N + V_{g,u}(R) + n\hbar\omega - E_v] \varphi_{g,u}^n(R) \\ - 1/2E\mu(R)[\varphi_{u,g}^{n-1}(R) + \varphi_{u,g}^{n+1}(R)] = 0. \end{aligned} \quad (6)$$

The weak-field, single-photon case is depicted by keeping only the zero-frequency Fourier component ($n = 0$) of $\chi_{g,v}(R, t)$ and the Fourier component ($n = -1$) of $\chi_{u,v}(R, t)$, denoted $\varphi_{g,v}(R)$ and $\varphi_{u,v}(R)$, respectively, leading to field-dressed diabatic (g, u) channels coupled equations:

$$\begin{aligned} [T_N + V_g(R) - E_v] \varphi_{g,v}(R) - 1/2E\mu(R) \varphi_{u,v}(R) = 0, \\ [T_N + V_u(R) - \hbar\omega - E_v] \varphi_{u,v}(R) - 1/2E\mu(R) \varphi_{g,v}(R) = 0. \end{aligned} \quad (7)$$

v labels a specific solution of Eq. (7), involving both its eigenenergy E_v and corresponding eigenvector through its Fourier components $\varphi_{k,v}(R)$. The validity of such an approximation, critically quantifying field intensities compatible with a perturbative regime for the radiative interaction, is discussed later. Note that, although BO electronic states are considered, diabaticity refers here to channels prior to the introduction of field-induced couplings. Resonances are solutions with Siegert-type outgoing-wave boundary conditions [26] and have complex quasienergies E_v of the form $\text{Re}(E_v) - i\Gamma_v/2$, where Γ_v is the resonance width related to

its decay rate. We refer to complex scaling of the coordinate R as a computational method to deal with L^2 square-integrable resonance wave functions [27]. The potential energy curves for the ground $X(1s\sigma_g)$ and first excited $A(2p\sigma_u)$ states of H_2^+ and their transition dipole are taken from Bunkin and Tugov, presenting the advantage of being fitted by compact analytical functions [28]. On spectroscopic grounds some numerical discrepancies with more accurate potentials [29,30] can be observed, especially with the highest vibrational levels, and even for the total number of vibrational levels accommodated by the ground state (19 instead of 20). Moreover, highly accurate calculations [29,31] even predict up to three vibration-rotation levels for the first excited A state, which is clearly not the case of Bunkin and Tugov's analytical function, namely, a sum of two purely decaying exponential. But, once again we wish to emphasize that H_2^+ is but an example of a homonuclear diatomic, with the potentiality to be transposed to other systems, and our conclusions are not affected by a possible lack of spectroscopic accuracy. The propagation of the multichannel wave function is carried by an efficient algorithm based on the Fox-Goodwin method [32,33]. In the following, the label v designates both the field-free vibrational level and the laser-induced resonance originating from this vibrational state. The dynamics can similarly be described on field-dressed adiabatic V_{\pm} channels. Their associated potentials $V_{\pm}(R)$ are merely obtained by diagonalizing the 2×2 matrix of the single-photon-dressed potentials $V_g(R), V_u(R) - \hbar\omega$, with off-diagonal couplings $\mu(R)\sqrt{I}$. In the specific case of H_2^+ , the field-free BO potentials $V_{g,u}(R)$ asymptotically converge to a common dissociation limit, actually taken as the zero of energies [28]. The single-photon dressing produces a diabatic curve-crossing situation at internuclear distances R_c depending on the laser frequency $\hbar\omega$ (or wavelength λ); large values of R_c are reached when increasing λ .

We are looking for a FR resulting from the radiative interaction of the lowest discrete level $v_+ = 0$ accommodated by the upper adiabatic potential $V_+(R)$ and the dissociative continuum of the lower adiabatic potential $V_-(R)$, in an energy region close to zero and a wave function localized at large internuclear distances. Two laser parameters take part in such a determination, namely, the intensity I and the wavelength λ . A first step is to fix the intensity to an almost negligible value and search for large wavelengths such that $V_+(R)$ still accommodates at least a single vibrational bound level $v_+ = 0$. It should be noted that when we refer to ‘‘almost-zero-field intensity’’ we are actually addressing a hypothetical situation where the potential energy curves are field dressed (by the corresponding number of absorbed or emitted photons) but not radiatively coupled, as if the field intensity were zero. On practical grounds, this could be compatible with arbitrarily low (still not strictly zero) intensities ($I = 10^{-8}$ W/cm², to fix the ideas) which lead to the calculation of adiabatic curves $V_{\pm}(R)$, with an avoided crossing limited to a single point. This study can be conducted by referring to a semiclassical existence criterion of a discrete level to be accommodated in the upper adiabatic potential. The corresponding phase condition could be written as [34]

$$\int_{R_-}^{R_+} dR' \frac{2m}{\hbar} [E_{v_+} - V_+(R')]^{1/2} = \left(v_+ + \frac{1}{2} \right) \pi, \quad (8)$$

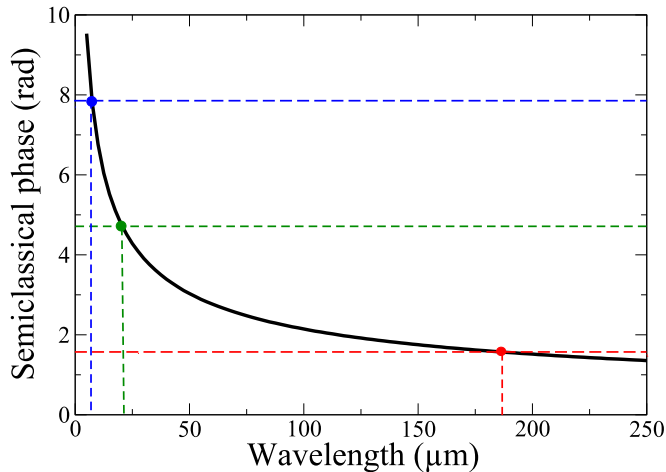


FIG. 1. Semiclassical phase (rad) as a function of the dressing laser wavelength (μm). The horizontal lines for $(v_+ + 1/2)\pi$ ($v_+ = 0$ lowest red-dashed, 1 middle green-dashed, and 2 uppermost blue-dashed line) indicate the semiclassical limits (dots) for the number of discrete states that are expected to be accommodated.

where R_{\pm} are, respectively, the right and left turning points of the vibrational level v_+ , the existence of which is under consideration. m is the system reduced mass. For $v_+ = 0$, if we look for an eigenenergy $E_{v_+} \simeq 0$ (i.e., close to the dissociation limit), reaching the value $\pi/2$ for the semiclassical phase, may necessitate very large values for the right turning point R_+ . Using the above-mentioned condition, we could determine an acceptable compromise between a photon dressing frequency (or corresponding wavelength λ) and a right turning point R_+ , such as to have a vibrational level $v_+ = 0$ of the upper adiabatic potential at a slightly negative energy. As an upper limit for the phase condition, we take $R_+ = R_{\text{max}}$, where $R_{\text{max}} = 40$ a.u. is the maximum extension of our spatial grid. In Fig. 1, the semiclassical phase defined by the left-hand side of Eq. (8) is plotted as a function of the laser wavelength λ . The horizontal dotted lines correspond to successive values of the right-hand side for $v_+ = 0, 1, 2$. The dots indicate the limiting values of λ for a number $(v_+ + 1)$ of discrete states that could be accommodated by the upper adiabatic potential $V_+(R)$. More explicitly, we observe that λ exceeding $180 \mu\text{m}$, the potential is too flat to accommodate any vibrational level. For $22 \mu\text{m} < \lambda < 180 \mu\text{m}$ or $10 \mu\text{m} < \lambda < 22 \mu\text{m}$, respectively, the occurrence of only a single or two vibrational levels is expected.

These values for wavelengths being taken as starting guesses, we address quantum calculations [Eq. (6)] for the accurate determination of FR energies. We are considering seven-channel calculations with almost zero-intensity THz laser fields. More precisely, these are the ones describing the reference single-photon Floquet block ($|g, n = 0\rangle$, $|u, n = -1\rangle$) together with two additional lower Floquet blocks for the two- and three-photon absorption, and an upper closed channel describing a single-photon emission process $|u, n = 1\rangle$. The variations of the FR positions as a function of laser wavelengths (taken in the region where a single bound level is still accommodated according to the semiclassical criterion of Fig. 1) are indicated in Fig. 2. The grid is taken large enough to account for the full spatial extension

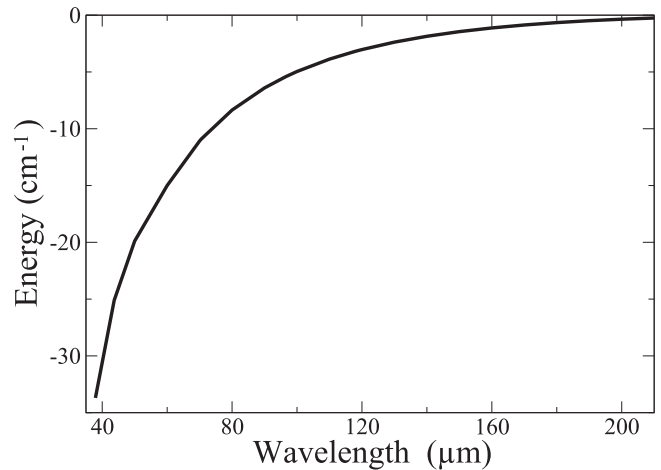


FIG. 2. Quasibound Feshbach resonance energy (cm^{-1}) as a function of the dressing laser wavelength (μm), extracted from a seven-channel adiabatic calculation, assuming almost zero-field intensity.

of the near-dissociation-threshold Feshbach wave function. For these full-quantum calculations, the parameters which are retained are $R_{\text{min}} = 0.5$ a.u. and $R_{\text{max}} = 100$ a.u. The step size $h = 0.005$ a.u. is small enough for a 20-points per channel description of the $v = 18$ vibrational function. The wiggling upper adiabatic potentials resulting from seven-channel calculations are illustrated for several wavelengths (and almost zero intensity) in Fig. 3 (left panel). They are characterized by three crossing points which are positioned according to the photon frequency in a multiphoton-dressed picture. These correspond to single-photon, two-photon, and three-photon absorptions, leading to two potential wells separated by a barrier. The wave functions of the $v_+ = 0$ levels supported by these potentials are displayed in Fig. 3 (right panel). It is important to notice that the almost zero-intensity FR wave functions are well displayed within internuclear distances not exceeding $R = 40$ a.u. and their maximum amplitudes are extending from about $R = 10$ to 15 a.u., that is well beyond the right turning point of the highest bound vibrational level $v = 18$. It is also worth noticing that their short-distance decreasing part does not much depend on the adiabatic potential wiggling structure, at least for these wavelengths. This is a consequence of the two-photon crossing barrier hard to penetrate.

Finally, Fig. 4 fully illustrates the specific case of $\lambda = 118 \mu\text{m}$ taken as an upper limit for the laser wavelength in this work. The figure displays in its main panel the long-range part of the seven adiabatic curves (at almost zero intensity) with the corresponding one-, two, three-photon crossings. The initial channel is the one asymptotically reaching the zero-energy dissociation threshold (as the ground diabatic state V_g). The inset shows an enlargement of this adiabatic potential which accommodates but a single vibrational level. Actually this is obtained for an eigenenergy $E_{v_+=0} = -3.2 \text{ cm}^{-1}$ (close to the dissociation threshold). The spatial grid extension is large enough to accurately describe the long tail of the corresponding wave function. The maximum probability density is at about $R = 13$ a.u. The next step is the actual calculation of variable intensity field-induced FR generated by this vibrational level, using a Floquet single-photon

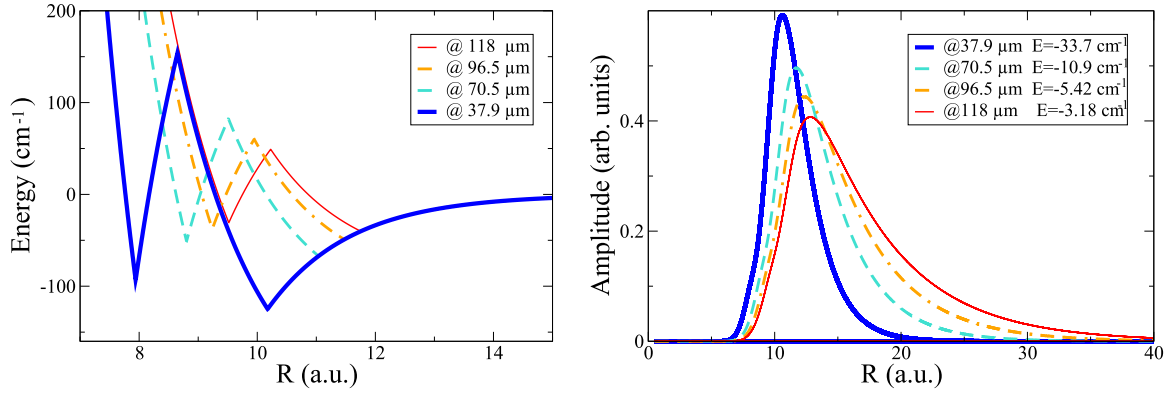


FIG. 3. Seven-channel adiabatic calculations with almost zero-field intensity. Left panel: wiggling adiabatic potentials (in cm^{-1}) for different THz laser wavelengths. Right panel: corresponding box-normalized quasibond Feshbach resonance wave functions as a function of R (a.u.). The color code is the same for both panels (thick solid blue for $\lambda = 37.9 \mu\text{m}$; dashed turquoise for $\lambda = 70.5 \mu\text{m}$; dashed-dotted orange for $\lambda = 96.5 \mu\text{m}$; and thin solid red for $\lambda = 118 \mu\text{m}$).

approximation. For this we need a precise determination of the critical laser intensity below which we are in the single-photon oasis (perturbation model). This could be done by referring to a criterion involving the intensity limit for the single versus multiphoton regimes, based on $|V_{\text{int}}/\hbar\omega| \ll 1$ [35]. The radiative interaction V_{int} is nothing but $V_{\text{int}} = \mu\sqrt{I}$. The corresponding maximum energy splitting between the two adiabatic curves, at the avoided crossing position R_c , is given by

$$\max_{R=R_c} [2V_{\text{int}}(R)] = 2\mu(R_c)\sqrt{I}. \quad (9)$$

As for the energy difference $\Delta E = 2\hbar\omega$ between subsequent Floquet blocks, it is given by

$$\min_{R=R_{\text{max}}} [\Delta E] = 2\frac{1}{\lambda}. \quad (10)$$

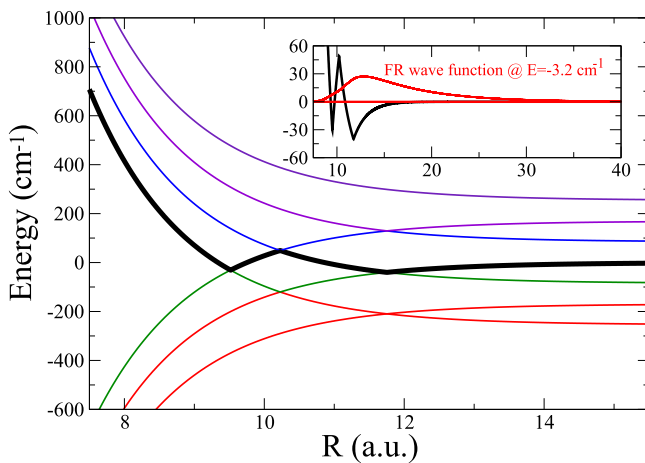


FIG. 4. Seven-channel adiabatic potentials (in cm^{-1} units) for $\lambda = 118 \mu\text{m}$ at large internuclear distances R (a.u.) for almost zero-field intensity. The thick solid black curve is the one asymptotically going to zero (as the ground diabatic state). The inset shows an enlargement of this potential which accommodates the FR at energy $E_{v_+=0} = -3.2 \text{cm}^{-1}$, together with its box-normalized wave function.

The ratio q between these quantities is then $q = 2\mu(R_c)\sqrt{I}\lambda/2$. Its critical value $q = 1$ finally leads to a critical intensity I_c ,

$$I_c = \frac{1}{\mu^2(R_c)\lambda^2}, \quad (11)$$

above which the laser field should be considered strong enough to induce nonlinear multiphoton effects. Figure 5 gives the variations of I_c as a function of λ for $\mu(R)$ calculated at two typical asymptotic internuclear distances $R = 30$ and 40 a.u. For a given λ , intensities less than the critical one (i.e., below the corresponding curve) have to be taken as leading to a single-photon absorption accounted for, by using only two potential curves $V_g(R)$ and $V_u(R) - \hbar\omega$, without the need of introducing additional channels to describe multiphoton processes. It is also interesting to note how the residual nonadiabatic couplings ϕ depend on the laser peak intensity for the single-photon versus multiphoton cases [35,36]. In the single-photon limit ($I < I_c$), where a diabatic representation is

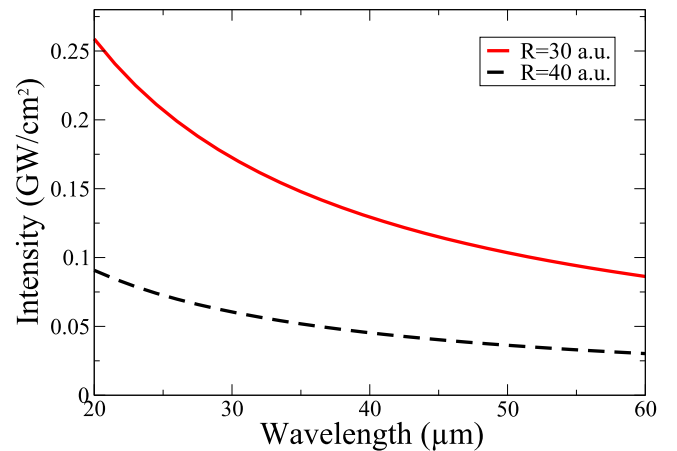


FIG. 5. Critical intensities (GW/cm^2) above which the single-photon perturbation regime is no more valid, as a function of laser wavelengths (μm) for two asymptotic internuclear distances $R = 30$ a.u. (upper solid red curve) and $R = 40$ a.u. (lower dashed black curve).

the most relevant, one has

$$\phi = \frac{V'_{\text{int}}(R)}{\hbar\omega} = \frac{\sqrt{I}}{\hbar\omega} \mu'(R), \quad (12)$$

which leads to an increasing behavior with intensity (primes indicate R derivatives). On the contrary, in the multiphoton regime ($I > I_c$), where an adiabatic representation is preferentially referred to, the nonadiabatic coupling turns out to be

$$\phi = \frac{\hbar\omega}{4} \frac{1}{\mu\sqrt{I}} \frac{d}{dR} \ln V_{\text{int}}(R) \quad (13)$$

a decreasing function of intensity. This is also why the stronger is the field and better will be the adiabatic representation with less coupled channels.

B. Critical determination of laser characteristics

The challenge is to find resonances which do not pertain to the class of short-range diabatic ones originating from the vibrational levels ($v = 0$ to 18) of the ground state with potential $V_g(R)$ and lying in the continuum of the field-dressed excited state with potential $V_u(R) - \hbar\omega$. These could be named as chemically bound molecular states (CBM) which are perturbatively modified by the external laser field. We emphasize that our objective is to produce long-range FRs which have a completely different interpretation. They are originating from the discrete levels with quantum numbers v_+ accommodated by the upper adiabatic potential $V_+(R)$ and nonadiabatically coupled to the continuum of the lower one $V_-(R)$. Especially if the diabatic curve crossing R_c occurs at large internuclear distances as compared with the field-free equilibrium distance, such resonances do not have their field-free counterpart among the 19 vibrational levels of H_2^+ . If, in addition, they can be laser controlled as to produce ZWRs, we would be in a position to provide a quasistable molecular system, where the chemical binding has been replaced by a field binding [which we name as laser bound molecule (LBM)]. When designing the laser, and more specifically its wavelength, we have to check the following points: (i) Due to charge-enhanced resonance in H_2^+ [19] the asymptotic transition dipole is a linearly increasing function $\lim_{R \rightarrow \infty} \mu(R) \propto R/2$. The consequence is an increasing radiative coupling with R . In particular, within a single-photon, two-channel description, the resulting adiabatic channels $V_{\pm}(R)$ will asymptotically diverge, resulting into large-distance FRs with positive energies above the dissociation limit, even for very low laser intensities. Only the introduction of other Floquet blocks (multiphoton effects) could attenuate (or better, suppress) such undesired behaviors. Actually, this turns out to be a major point for the choice of the laser wavelength. (ii) In a multichannel description, we have to check that the resulting adiabatic potential wiggling, if neglected (as in Fig. 6), has no noticeable effect on the accuracy. (iii) The validity of time-independent Floquet model rests on a cw-like laser (periodic field). Considering few cycles THz pulses, an approximate fulfillment of periodicity would require a long enough pulse duration, but still limited to avoid non-negligible rotational effects. (iv) A careful choice of the integration parameters for the close-coupled equations in relation with the particular shape of the long-range,

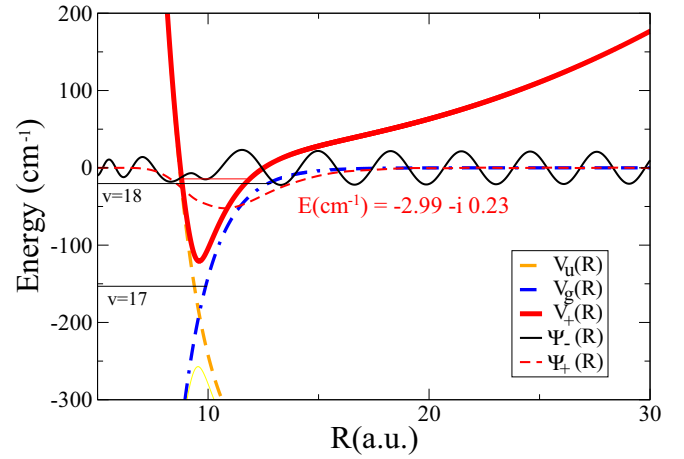


FIG. 6. Adiabatic $V_+(R)$ (thick, solid red curve) and diabatic V_g (blue dashed-dotted), V_u (orange dashed lines) potential energies (in cm^{-1}) as a function of R (a.u.), for an intensity of $0.65 \text{ GW}/\text{cm}^2$. The Feshbach resonance energy originating from $v = 18$ is $E(\text{cm}^{-1}) = -2.99 - i0.23$ (horizontal thin red line). The real parts of adiabatic channel components of its wave function (labeled Ψ_{\pm} in arbitrary units) are indicated as a thin dashed red line on channel V_+ , and as a black thin solid line on channel V_- .

large-extension FR should be conducted. These parameters could markedly differ from the standard diabatic resonance calculations. (v) Although laser intensities could be viewed as weak, on an absolute scale, they are expected to induce highly nonlinear effects, from middle infrared to THz wavelength regimes (as illustrated in Fig. 5). The convergence in terms of multiphoton effects (total number of Floquet blocks in the calculation) has to be carefully checked.

In summary, the choice of the laser wavelength results from a subtle compromise. Clearly, a laser in the THz regime ($\lambda = 118 \mu\text{m}$) as the one considered up to here for exploratory calculations produces an avoided curve crossing in the field-dressed adiabatic states at large internuclear distances (close to $R = 13$ a.u.) and a resulting FR close to the dissociation threshold, at very low intensities (see Fig. 4, where the result is illustrated at almost zero-field intensity). However, it is important to note that for this almost zero-intensity regime, the adiabatic representation of the resulting FR does not present any physical interest due to remaining very large nonadiabatic couplings [Eq. (13)]. Moreover, our ultimate goal is to laser control this resonance to promote it into a ZWR, such as to produce a LBM. At such large-distance avoided curve crossings, even a very moderate increase of the field strength will induce large radiative couplings due to the asymptotic behavior of the charge-resonant transition dipole, resulting in important multiphoton effects. A large number of additional Floquet blocks should then be taken into account, both for the proper description of the highly nonlinear behavior of the FR (convergence of the close-coupled equations) and also for a correct asymptotic representation of the dissociation channels. Not only the numerical approach but also the interpretation would then be severely impacted. Moreover, when attempting the production of a ZWR, we of course are in a nonlinear regime, but preferentially with a moderate multiphoton process. An important number of Floquet blocks may offer

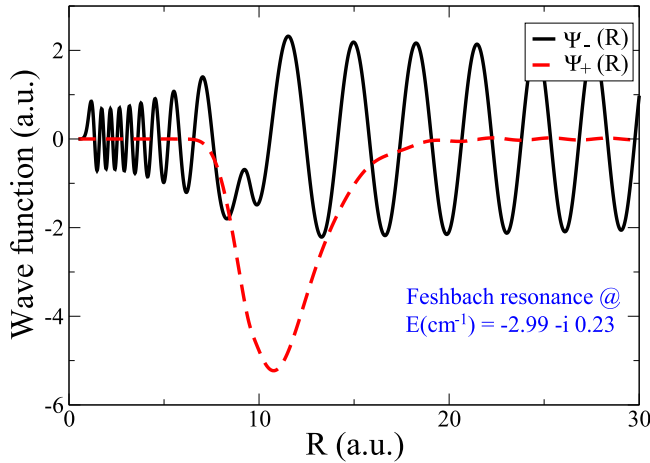


FIG. 7. Real parts of the $v = 18$ Feshbach resonance wave function (in arbitrary units) as illustrated through its components on the adiabatic channels (same as in Fig. 6, but with a different scale). Red dashed line for the V_+ , black solid line for the V_- channel components.

additional decay channels, the control of which goes beyond our present models for the ZWR description. Following several attempts to fulfill the requirements of the different aspects of this compromise, and also to secure a semiclassical energy arrangement which is a basic criterion for ZWR, we finally fixed our choice, in the following part of this study, to a 100-ps pulse duration middle infrared laser field, with a wavelength of $\lambda = 25 \mu\text{m}$ (frequency $\omega = 400 \text{ cm}^{-1}$, i.e., 12 THz) which actually produces a curve-crossing situation close to $R_c = 9.6 \text{ a.u.}$ The peak intensity is chosen of the order of $I = 1 \text{ GW/cm}^2$, which, according to Fig. 5, is already strong enough to induce nonlinear responses and multiphoton effects.

III. RESULTS FOR LONG-RANGE FESHBACH RESONANCES AT $\lambda = 25 \mu\text{m}$

A. Role of charge resonance enhanced transition dipole

We first examine the role of the asymptotically increasing charge resonance enhanced transition dipole in a two-channel description, with an intensity of $I = 0.65 \text{ GW/cm}^2$, still moderate but with the potentiality to induce nonlinear responses. The corresponding diabatic and adiabatic potentials are illustrated in Fig. 6, together with the corresponding wave functions. The increasing behavior of $\mu(R)$ plays a determinant role, at internuclear distances typically of the order of $R = 12 \text{ a.u.}$, even for this relatively modest intensity. The potential energies are severely modified by an important increase from their expected asymptotic behaviors. As a consequence, even for slightly stronger fields, this would result in undesired FRs with positive energies, above the dissociation threshold. Figure 7 illustrates, on an enlarged scale, the components of the corresponding FR on the adiabatic channels V_{\pm} . Its complex eigenenergy is $E(\text{cm}^{-1}) = -2.99 - i0.23$, close to, and below the dissociation threshold (taken as the origin of energies in this field-dressed potential representation). It is worthwhile noting that for the intensity under consideration,

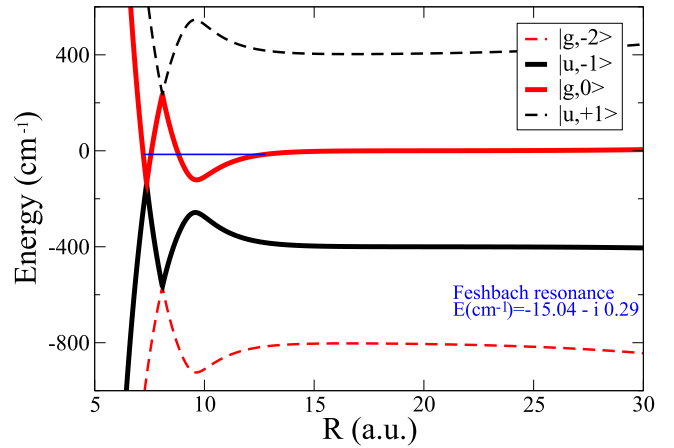


FIG. 8. Adiabatic potentials of a three-block, six-channel Floquet model, for a laser wavelength $\lambda = 25 \mu\text{m}$ and an intensity $I = 0.65 \text{ GW/cm}^2$. Only the four innermost channels are illustrated. The labeling is the one of the asymptotic diabatic limits. The solid thick lines correspond to the upper V_+ (red) and the lower V_- (black) potentials, as discussed in the two-channel model. The Feshbach resonance is at $E(\text{cm}^{-1}) = -15.04 - i0.29$.

the imaginary part of the resonance wave function can be safely neglected. Its component on the lower adiabatic channel V_- is oscillating in the inner region ($R < 9.6 \text{ a.u.}$), still borrowing (as a reminiscence) its nodal structure from the vibrational state $v = 18$. For larger distances ($R > 10 \text{ a.u.}$) a regular oscillating pattern is observed in relation with the continuum part of the corresponding channel potential. A slight decrease of periodicity is also observed once again due to the role of $\mu(R)$ which locally enhances the energy decrease of $V_-(R)$. But, more interestingly, a high-amplitude, well-peaked component is observed on the upper adiabatic channel V_+ . With its maximum amplitude around $R = 11 \text{ a.u.}$, this wave function does obviously not pertain to the class of diabatic resonances. Its tiny oscillations (for $R > 15 \text{ a.u.}$) are in phase opposition with those of the V_- component, a contamination effect between the components (nodes are for the same position in all channels).

We now move to a six-channel description by introducing two additional Floquet blocks to describe in a symmetrically balanced way multiphoton absorption and emission processes, with respect to the previous single-photon reference block. At this stage, our purpose is rather to examine how to suppress (or at least slow down) the energy increase of the two single-photon reference channels V_{\pm} at large distances, as resulting from the charge resonance enhanced transition dipole. The role of additional Floquet blocks for multiphoton effects (convergence issues) will be considered later. The resulting adiabatic potentials are illustrated in Fig. 8. When diagonalizing the 6×6 diabatic potentials matrix with the corresponding off-diagonal radiative couplings, the extreme eigenvalues will push the intermediate ones, thus avoiding their divergence. It is interesting to note that this argument works satisfactorily at least up to internuclear distances of about $R = 30 \text{ a.u.}$ We actually observe an almost zero-energy asymptotic value for the upper adiabatic channel $V_+(R)$ of the reference block accommodating the Feshbach resonance,

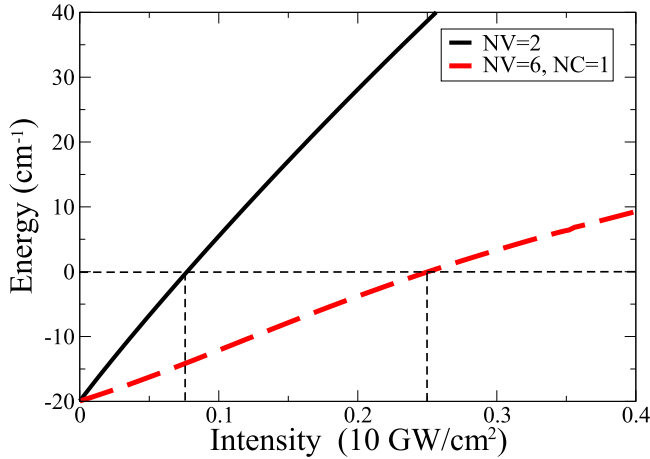


FIG. 9. Energy of the Feshbach resonance (in cm^{-1} units) as a function of intensity (in $10 \text{ GW}/\text{cm}^2$ units). The solid black and red dashed lines are, respectively, for two- versus six-channel calculations, with a laser wavelength of $\lambda = 25 \mu\text{m}$.

whereas $V_-(R)$ goes to $\simeq -400 \text{ cm}^{-1}$, actually corresponding to the $25\text{-}\mu\text{m}$ -photon energy dressing. The effect of the charge resonance enhanced transition dipole is already observable for the two-photon absorption ($|g, -2\rangle$) or single-photon emission ($|u, +1\rangle$) channels, which asymptotically show values below or above their expected energy thresholds ($\pm 800 \text{ cm}^{-1}$, respectively). It is also interesting to note the wiggling behavior (as already observed for other wavelengths, in Fig. 3) resulting from the avoided crossing positions for single- ($R = 9.6 \text{ a.u.}$), double- ($R = 8.1 \text{ a.u.}$), and triple- ($R = 6.9 \text{ a.u.}$) photon processes. For clarity, it should be noted that only the single-photon avoided crossing is related to a direct radiative process $|g, n = 0\rangle \rightarrow |u, n = -1\rangle$, all higher-photon processes involve sequential absorption, *e.g.*, $|g, n = 0\rangle \rightarrow |u, n = -1\rangle \rightarrow |g, n = -2\rangle$, that we name double-photon process. The consequences on FR energies, as evaluated for different laser intensities, are analyzed in Fig. 9. When limiting to a two-channel model, intensities exceeding $0.75 \text{ GW}/\text{cm}^2$, are already leading to a resonance position above the dissociation threshold (with positive energy). It is interesting to note that, when moving to a six-channel description to accommodate resonances below the dissociation threshold, this range of intensity can be extended up to $2.55 \text{ GW}/\text{cm}^2$.

B. Multiphoton issues affecting Feshbach resonances

We now return to the role of a multichannel description for examining the nonlinear response resulting from multiphoton processes undergone by the molecule when subjected to nonperturbative radiative interactions (strong-field effects). In Fig. 10, we plot the FR rates as a function of laser intensities. These are calculated solving close-coupled equations with the inclusion of multiphoton dynamics, through additional Floquet blocks describing both absorption and emission processes, up to convergence.

The single-photon process is described by the reference Floquet block involving but two diabatic channels, namely, $|g, 0\rangle$ and $|u, -1\rangle$. This model is depicted in Fig. 10 by the

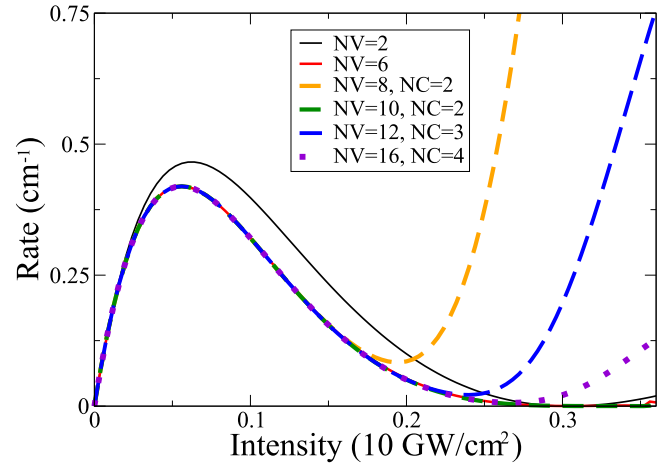


FIG. 10. Feshbach resonance rates (in cm^{-1} units) as a function of the laser intensity (in $10 \text{ GW}/\text{cm}^2$ units) for increasing number of channels describing multiphoton processes at $\lambda = 25 \mu\text{m}$. NV designates the total number of channels (absorption and emission), NC the one of photon emission. Single-photon rates are given by the solid black curve ($NV = 2$). An almost converged result is obtained for $NV = 16$ and $NC = 4$, displayed as violet dots.

label $NV = 2$ (NV being the total number of channels). Up to intensities of about $0.1 \text{ GW}/\text{cm}^2$, the rate Γ is increasing linearly with respect to the intensity. This is the so-called perturbative regime, where the diabatic channels hold the fingerprints of the molecule. The corresponding FRs are directly related to field-free vibrational states of the ground electronic potential $V_g(R)$ which are radiatively and weakly coupled to the dissociative continuum of the field-dressed excited electronic potential $V_u(R) - \hbar\omega$. In particular, the FR we have in mind is the one originating from $v = 18$. This describes a situation we can name as a chemically bound quasistable molecule (CBM), its lifetime being proportional to $1/\Gamma$. The subsequent nonlinear (nonperturbative) behavior of Γ shows first a slower increase, with saturation at intensities of about $0.65 \text{ GW}/\text{cm}^2$. For stronger field intensities, we observe a regular decrease of Γ . This is a well-known basic mechanism depicted as vibrational trapping [12–14]. Actually, the fingerprints of the molecule move from the vibrational levels of the diabatic potential $V_g(R)$ to those of the upper adiabatic potential $V_+(R)$ which are nonadiabatically coupled to the continuum of $V_-(R)$. As has been previously shown, these nonadiabatic couplings, contrary to the diabatic ones, are decreasing with increasing intensities [Eq. (13)]. The stronger the field, the better is the efficiency of the vibrational trapping mechanism. Accordingly, the vibrational level v_+ accommodated by $V_+(R)$ is less coupled to its corresponding dissociative continuum $V_-(R)$, the resulting FR showing an increasing lifetime. Although the model is based on diabatic channels [the close-coupled equations (6) actually rest on a diabatic representation], an adiabatic description is better suited for the interpretation. The most important and unexpected behavior is observed for a critical field intensity of $3.04 \text{ GW}/\text{cm}^2$, for which the rate is almost strictly zero. This very interesting peculiarity which has been named zero-width resonance (ZWR) is not a consequence of a regular decrease of the nonadiabatic

coupling [as could be seen from a logarithmic scale representation $\log \Gamma(I)$ resulting in very sharp dips [8,37]]. It has in particular been shown that the responsible mechanism is a two-adiabatic-channel destructive interference that happens for a critical choice of two laser parameters, wavelength λ_{ZWR} and intensity I_{ZWR} [38]. Once again, it is worthwhile noting that the corresponding Feshbach-type ZWR resonance does not pertain to the class of diabatic resonances originating from one of the field-free vibrational levels, but has rather an adiabatic interpretation as originating from a field-induced vibrational level v_+ accommodated by the upper adiabatic channel potential $V_+(R)$. Even more importantly, for specific laser parameters, this FR merges into a ZWR, i.e., a bound state with some peculiarities: wave function located at large internuclear distances and energy positioning close to the dissociation threshold. The quasistable highly stretched molecule which is formed can only exist as long as the laser is switched on with its characteristic parameters, but still in a rather robust way. We are designating this as a laser bound molecule (LBM) as opposite to a chemically bound molecule (CBM). For the specific case of H_2^+ , as already mentioned, it should be noted that the occurrence of at least one vibrational level $A(v=0)$ accommodated by the excited state potential, due to long-range forces, has been predicted [39] and later confirmed by nonrelativistic quantum calculations going beyond BO approximation [29–31]. This, of course, is by no means the LBM we are referring to here, not only because the potential function we are using does not accommodate such a level, but the LBM wave function results from an interference mechanism involving both the ground and excited states, which obviously is not the case of $A(v=0)$.

As we have seen, highly nonlinear responses of the molecular system to the external laser field can be observed even without referring to multiphoton processes. Actually, the basic mechanisms at the origin of such nonlinearities, namely bond softening or vibrational trapping, are in relation with important modifications of the dressed adiabatic potential energies already present in the reference Floquet block. Multiphoton effects should, however, be properly described in order to get converged results. This is done by progressively introducing additional Floquet blocks. The periodicity of the Brillouin zone is based on an energy difference of $\Delta E = 2\hbar\omega$ [Eq. (10)], such that the two channels making up a Floquet block cannot be separately considered. In other words, if we add channels describing absorption or emission, this should be done through extra two-channel Floquet blocks symmetrically disposed with respect to the reference single-photon block. If NC denotes the number of closed emission channels (i.e., the ones above the dissociation limit in the field-dressed molecule picture, namely, $|u, +1\rangle, |g, +2\rangle, |u, +3\rangle, \dots$), we must in principle fulfill the condition $NV = 2(2NC + 1)$. The results are displayed in Fig. 10. The cases where the Brillouin periodicity is assumed ($NV = 2, 6, 10$), the rates Γ present the expected smooth decrease, up to intensities close to I_{ZWR} . For the others, nonphysical increasing values are obtained for intensities stronger than 2 GW/cm^2 . From Fig. 10 we also observe that multiphoton effects start to play a role for intensities above 0.2 GW/cm^2 resulting into lower rates (more efficient vibrational trapping). The convergence is almost reached with a six-channel ($NV = 6, NC = 1$) description. Finally, the

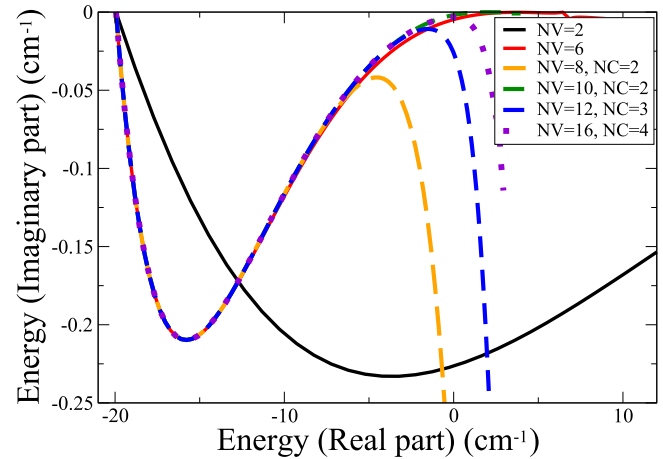


FIG. 11. Feshbach resonance trajectories at $\lambda = 25 \mu\text{m}$ in the complex energy plane (imaginary versus real parts in cm^{-1}) with the field intensities referred to in the abscissa of Fig. 10. The single-photon process ($NV = 2$) is illustrated by the solid black line. Same notations as in Fig. 10, for the multiphoton processes ($NV > 2$).

critical intensity for the ZWR is only slightly removed for a higher intensity 3.04 GW/cm^2 . To be complete, we have to say that, mathematically speaking, the ZWR we are referring to has a full interpretation solely in a two-channel description. Additional absorption channels offer extra dissociation partial rates which will simply add to the (zero) one of the reference block [40]. Even though the multiphoton rate is not strictly zero, one can see from Fig. 10 that for the intensity regime in consideration it remains close to this value. FRs are also characterized by their energy positioning. In Fig. 11 we examine their trajectories in the complex energy plane with increasing field intensities. The differences between single-photon ($NV = 2$) and multiphoton processes ($NV > 2$) are even more marked for these trajectories. The field-free situation corresponds to the real energy of the 18th vibrational level of $V_g(R)$, $E_{v=18} = -20.23 \text{ cm}^{-1}$, slightly below the dissociation threshold taken as the origin of energies. In the single-photon ($NV = 2$) model, the undesired positive energies, in relation with the charge resonance enhanced transition dipole $\mu(R)$, occur for intensities exceeding 2.55 GW/cm^2 as already observed in Fig. 9. This situation dramatically changes with increasing number of channels. Almost all intensities up to the ones close to the ZWR produce long-lifetime FRs (Γ less than 10^{-3} cm^{-1}) which are positioned below the dissociation threshold, as expected. In this respect, the role of multiphoton processes is even more important than for the rates, for which a six-channel ($NV = 6, NC = 1$) description seems enough converged for the intensity regime under consideration.

IV. ZWR AND LASER BOUND MOLECULE CHARACTERIZATION

A. ZWR in terms of an interference mechanism.

We are hereafter generalizing Child's semiclassical approach [20,21,38] to a multichannel description of the ZWR. This is done by building two adiabatic potentials $V_{\pm}^{\text{sc}}(R)$ which will accommodate two energy levels that we should bring

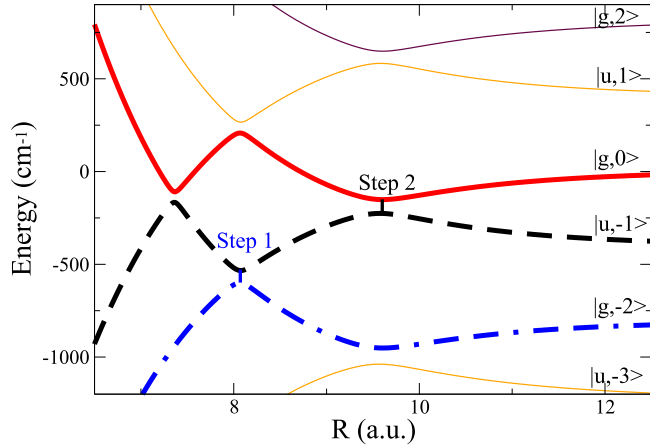


FIG. 12. Potential energy curves (in cm^{-1} units) from a six-channel ($NV = 6$, $NC = 1$) adiabatic model with a laser of wavelength $\lambda = 25 \mu\text{m}$ and intensity $I = 0.2 \text{ GW/cm}^2$. The channels are labeled in terms of their asymptotic diabatic counterparts. The three adiabatic potentials that play a part in the generalized semiclassical model are depicted in thick lines (dotted dashed blue, dashed black and solid red). It is important to note that two potential steps have been introduced for the single (step 2, at $R = 9.6$ a.u.) and two-photon (step 1, at $R = 8.1$ a.u.) avoided crossings (step 1 being the novelty with respect to Child's original model).

into coincidence through a laser control. It is precisely this coincidence condition (also taking into account an additional phase factor χ) which is required by the semiclassical theory of destructive flux interference among these adiabatic channels. The two potentials in consideration are built piecewise from the adiabatic ones illustrated in Fig. 12 and labeled in conformity with their asymptotic limits. More precisely, the lower adiabatic potential $V_-^{\text{sc}}(R)$ follows, up to the two-photon diabatic crossing point ($R = 8.1$ a.u.), the adiabatic channel $|g, -2\rangle$. At $R = 8.1$ a.u., a step function (labeled step 1 in Fig. 12) leads to the adiabatic potential of channel $|u, -1\rangle$ which in turn is followed up to the single-photon diabatic crossing point ($R = 9.6$ a.u.). The generalization for the multiphoton process of Child's original model is precisely this additional step function (i.e., step 1). A second step function (labeled step 2, in Fig. 12) then leads to the adiabatic potential of channel $|g, 0\rangle$ which is followed up to the end of the grid. As for the upper adiabatic potential $V_+^{\text{sc}}(R)$, it is nothing but the adiabatic potential of channel $|u, -1\rangle$ up to $R = 9.6$ a.u., and then the one of $|g, 0\rangle$. Figure 13 shows the wave function of the piecewise lower adiabatic potential with its two local discontinuities in terms of the step functions of about 240 cm^{-1} height. The smooth behavior and regularity of the wave function with its 18 nodes shows that the algorithm does not suffer from any numerical convergence issues. This illustrates graphically the numerical validity of the multiphoton generalization which is attempted. In conformity with Child's original semiclassical model, this generalized version also leads to a ZWR obtained through a destructive interference mechanism controlled by specific laser wavelength and intensity parameters, which are tuned in such a way that two vibrational levels v and v_+ , with energies E_v^{sc} and $E_{v_+}^{\text{sc}}$, are

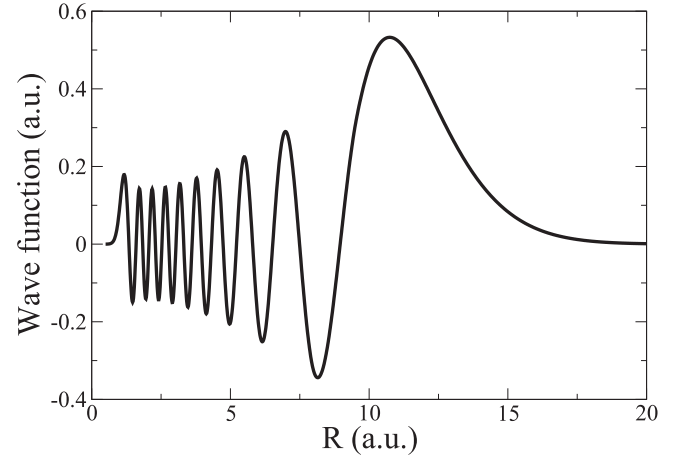


FIG. 13. The wave function (in arbitrary units) of the lower piecewise built adiabatic potential $V_-^{\text{sc}}(R)$ including the two step functions at $R = 8.1$ a.u. (two-photon absorption) and $R = 9.6$ a.u. (single-photon absorption) depicted, respectively, as step 1 and step 2 in Fig. 12, but now for an intensity $I = 3.6 \text{ GW/cm}^2$, the semiclassical estimate of I_{ZWR} .

brought in coincidence. More precisely, these energies are defined by the two quantization conditions

$$\int_{R_+^l}^{R^r} dR \frac{2m}{\hbar} [E_v^{\text{sc}} - V_-^{\text{sc}}(R, I)]^{1/2} = \left(v + \frac{1}{2}\right)\pi, \quad (14)$$

$$\int_{R_+^l}^{R^r} dR \frac{2m}{\hbar} [E_{v_+}^{\text{sc}} - V_+^{\text{sc}}(R, I)]^{1/2} + \chi(I) = \left(v_+ + \frac{1}{2}\right)\pi \quad (15)$$

with $v = 18$ (at $I = 0$) and $v_+ = 0$. R_+^l are the left turning points on V_{\pm}^{sc} and R^r the common right turning point, fixed in such a way that the integrand be a real-valued function. The phase χ is a function of the intensity-dependent Landau-Zener transition probability at the avoided curve crossing. Its full expression involves incomplete gamma functions [21,34]. It is interesting to note that $\chi(I)$ smoothly varies from $-\pi/4$ (-0.7854 rad) for zero-field intensity, up to -0.23 rad for $I = 4 \text{ GW/cm}^2$, which is our upper intensity limit. Actually, this variation of χ reveals to be crucial when matching $E_v^{\text{sc}}(I)$ and $E_{v_+}^{\text{sc}}(I)$, as displayed in Fig. 14. This demonstrates that, although not obvious for such wavelengths as sketched in introductory considerations, a theoretical support in terms of a two-channel destructive interference mechanism is provided for a ZWR produced through the couple of critical laser parameters ($\lambda = 25 \mu\text{m}$, $I = 3.6 \text{ GW/cm}^2$). We emphasize that these are actually rather good semiclassical estimates for quantum mechanically obtained values ($\lambda_{\text{ZWR}} = 25 \mu\text{m}$, $I_{\text{ZWR}} = 3.04 \text{ GW/cm}^2$) validating thus, in a *posteriori* way, the multichannel generalization of the model.

B. Laser bound molecule LBM characterization

In order to better characterize the laser bound quasistable molecular system LBM (as opposite to the usual chemically bound molecule, CBM), we now examine the peculiarities of the long-range FR supporting it. More precisely, the terminology LBM would apply for this state with a field intensity

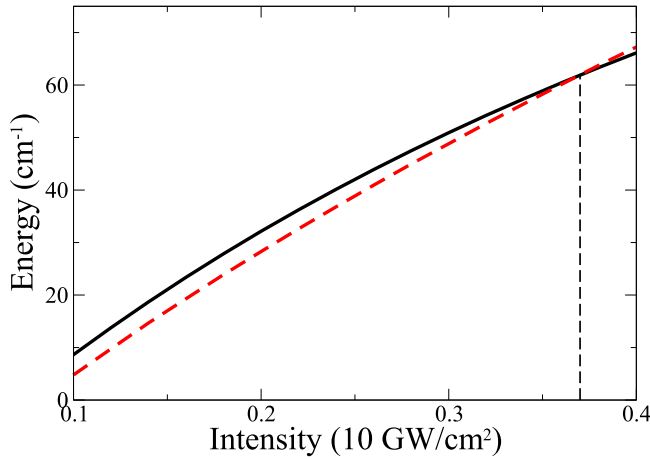


FIG. 14. Semiclassical coincidence condition for the energies (in cm^{-1} units) of the double-step piecewise lower adiabatic $v = 18$ level E_v^{sc} in solid black and the upper adiabatic $v_+ = 0$ level, with its phase correction $E_{v_+}^{\text{sc}}$ in dashed red, as a function of laser intensity (in $10 \text{ GW}/\text{cm}^2$ units). The two almost parallel curves intersect at about $3.6 \text{ GW}/\text{cm}^2$, which is the semiclassical estimate for $I_{\text{ZWR}} = 3.04 \text{ GW}/\text{cm}^2$ obtained from quantum calculations.

$I_{\text{ZWR}} = 3.04 \text{ GW}/\text{cm}^2$, producing the long-lived ZWR. Three observables are analyzed:

(i) The LBM wave function $\Phi^F(R)$. Figures 15 and 16 display all the six components of $\Phi^F(R)$ on the channels of the ($\text{NV} = 6, \text{NC} = 1$) model illustrated in Fig. 12, and for the ZWR intensity. It is worthwhile noting that for this particular intensity, the FR is actually a bound state with strictly real-valued wave-function components. The strictly bound character of the ZWR is clearly evidenced by the square-integrable (box-normalized) wave functions, without any long-range oscillation which could be interpreted as reminiscences of the open (continuum) channels. In both representations, but especially in the adiabatic one, one observes

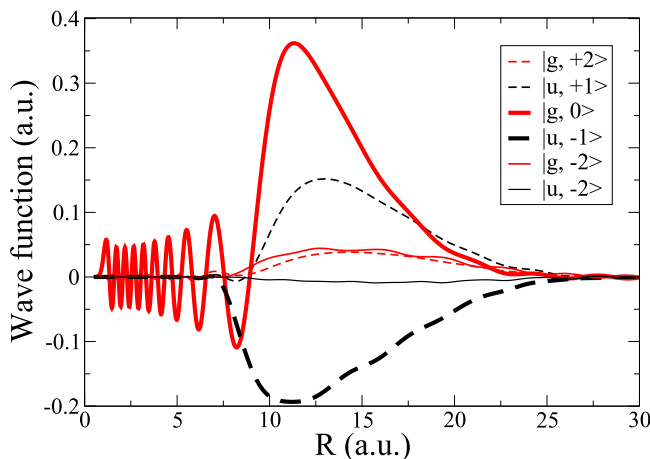


FIG. 15. The six-channel box-normalized wave-function components of $\Phi^F(R)$ (in arbitrary units) for the ZWR intensity $I_{\text{ZWR}} = 3.04 \text{ GW}/\text{cm}^2$, in diabatic representation, with its proper labeling. The almost zero imaginary parts of the wave-function components on all channels are not displayed.

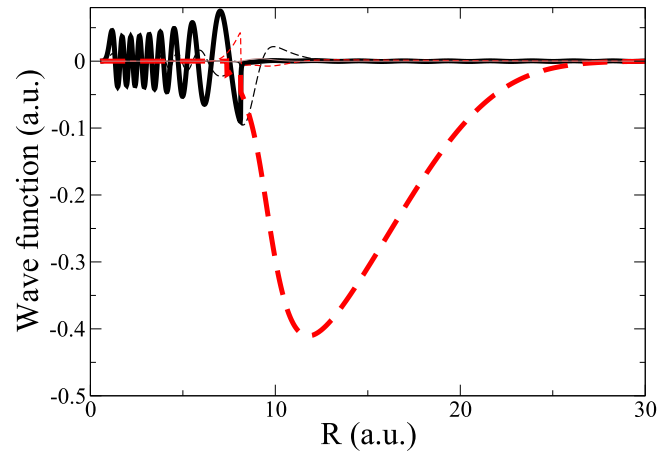


FIG. 16. Same as in Fig. 15, but for the adiabatic representation.

the main amplitude peak on the channel which asymptotically corresponds to $|g, 0\rangle$ and accommodates the ZWR (as an adiabatic condensation). Once again, it is important to note that such wave functions sharply peaked at large internuclear distances have no counterparts in terms of field-free vibrational wave functions. Only very attenuated signatures of $v = 18$ bound state can be seen in appropriate channels at short distances. It is in this respect that they markedly differ from CBM and open the interpretation of LBM.

(ii) Average values of $\langle R \rangle$. Such averages can first be evaluated for the class of states building up the CBM. These are the field-free vibrational bound levels $\chi_{gv}(R)$ ($v = 0$ to 18) of the ground-state potential $V_g(R)$. We are using the following definition:

$$R_v = \frac{|\langle \chi_{gv} | R | \chi_{gv} \rangle|}{\|\chi_{gv}\|^2}. \quad (16)$$

The results are collected in Fig. 17. A smooth and rather modest increase is observed from the equilibrium value of

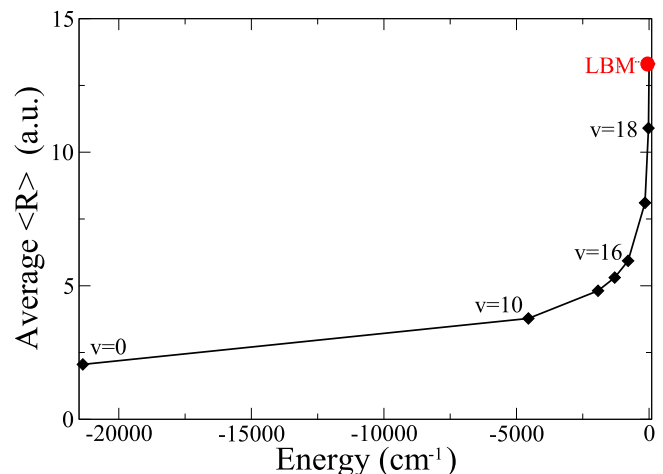


FIG. 17. Average values of R ($\langle R \rangle$ in a.u.) as a function of energy (in cm^{-1}) for the ground V_g state vibrational levels ($v = 0$ up to 18) represented by black diamonds. LBM in red dot stands for the laser bound molecule ($v_+ = 0$). The continuous line is only for guiding purpose.

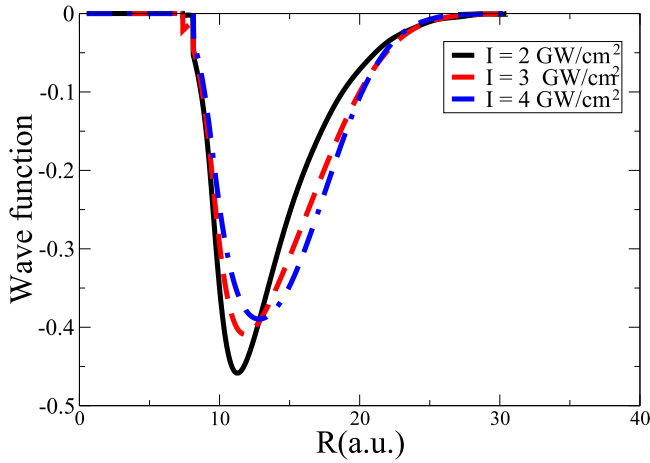


FIG. 18. Normalized main components (in arbitrary units) of the adiabatic long-range FR wave functions for three laser intensities. The one in dashed red corresponds to I_{ZWR} as denoted LBM in Fig. 17. The two others are for $I = 2 \text{ GW/cm}^2$ (solid black) and $I = 4 \text{ GW/cm}^2$ (dashed-dotted blue).

$R_0 = 2 \text{ a.u.}$, up to $v = 10$ where $R_{10} = 3.78 \text{ a.u.}$ For levels $v > 15$, due to important anharmonicity, the increase becomes much larger with the molecule stretched up to an average value $R_{18} = 10.9 \text{ a.u.}$ This is what we typically have in mind when addressing to a chemical binding with the highest possible vibrational excitation. To quantitatively point out the difference with what could be obtained when addressing quasistable molecules with laser-induced binding forces (LBM), we calculate the average internuclear distance referring to the long-range FR:

$$R^F(I) = \frac{|\langle \Phi_{v_+}^F(I, R) | R | \Phi_{v_+}^F(I, R) \rangle|}{|\Phi_{v_+}^F(I, R)|^2}, \quad (17)$$

where $\Phi_{v_+}^F(I, R)$ is the main adiabatic component of the FR as obtained from the six-channel calculation illustrated in Fig. 18 for an intensity corresponding to the ZWR. For other intensities, the Feshbach wave function is obviously no more real. However, as its imaginary part is rather small, we avoid the c -dot product [41] when calculating the integrals building up $R^F(I)$ [Eq. (17)], by only considering its real part. Figure 18 collects $\Phi_{v_+}^F(I, R)$ for three different intensities, including I_{ZWR} . We observe together with a slight flattening a shift toward larger internuclear distances of the maximum amplitude. This of course is well interpreted when referring to the intensity-dependent modifications of the main channel adiabatic potential accommodating the FR, as illustrated in Fig. 8. Finally, Fig. 19 displays, as a function of energy, the average values of R for both the field-free vibrational levels and for the laser-induced FRs at different field intensities. It is interesting to note that molecular stretching up to $R^F = 13.8 \text{ a.u.}$ is obtained for the strongest field in consideration $I = 4 \text{ GW/cm}^2$. The ZWR leads to $R^F = 13.33 \text{ a.u.}$ which is notably larger than the highest value $R_{18} = 10.9 \text{ a.u.}$ obtained for the field-free molecule. Here again the conclusion is that the long-range FRs which are obtained actually show an average value for the stretching exceeding 30% as compared to the maximum value obtained with the highest excited field-free

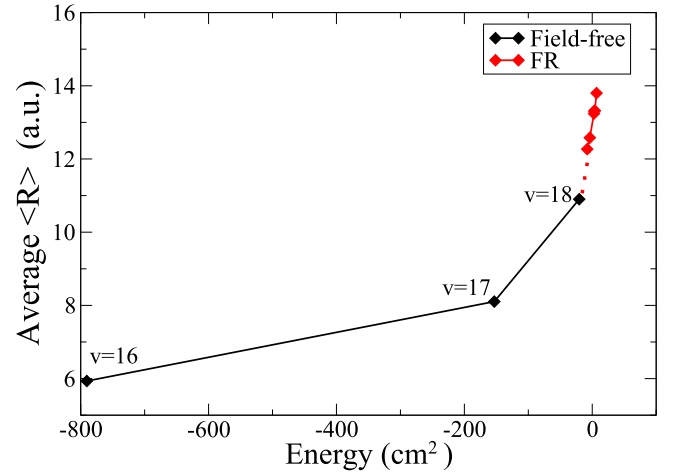


FIG. 19. Average values of R ($\langle R \rangle$ in a.u.) for upper ($v > 15$) field-free vibrational states building up the CBM and for the long-range FRs at various laser intensities. The one corresponding to I_{ZWR} illustrates the LBM as already mentioned in Fig. 17.

molecule. In particular, for the laser parameters corresponding to the ZWR, it shows that we have successfully achieved our objective to produce a stable laser bound molecule (LBM) with probability density at large internuclear distances.

(iii) The overlaps of $\Phi^F(I, R)$ with the field-free vibrational levels. We are now interested in the dynamical role the ZWR may play during a collision process to temporarily trap the incoming collisional wave packet. This could be done by an adiabatic switching of the laser pulse (using for instance a sine-square rising front from $I = 0$ to $I_{\text{ZWR}} = 3.04 \text{ GW/cm}^2$) that allows the building up of the ZWR during the time where the collisional wave packet reaches the long-range avoided curve-crossing region. At this time and all over the pulse duration, part of the collisional wave packet (trapped or not by the ZWR) will have some components mainly on the highest excited vibrational levels (say $v = 16, 17$, and 18), which actually behave, in turn, as finite lifetime resonances due to the ongoing laser excitation. The relatively short-range wave function of such resonances being not too sensitive to long-distance adiabatic potential energies [modifications due to $\mu(R)$], a simple two-channel calculation is assumed to be enough for the evaluation of their widths, or their lifetimes. For the specific intensity leading to the ZWR, much contrasted lifetimes are obtained, namely, $\tau_{18} = 510^5 \text{ ps}$, $\tau_{17} = 0.4 \text{ ps}$, and $\tau_{16} = 78.3 \text{ ps}$. As a reminder, for this laser intensity the ZWR has, in principle, an infinite lifetime. This means that for a laser pulse with a plateau value at I_{ZWR} , a duration of about 78 ps will be enough to dissociate the two neighboring resonances $v = 17$ and 16 . This is in relation with the filtration strategy based on the ZWR that we have previously analyzed in a different context [42]. Following the plateau value, the laser pulse is adiabatically switched off (by a final sine-square decrease, for instance). During this time, we examine how the ZWR (or the collision wave packet which is trapped by it) is projected on its neighboring field-free vibrational states. At this end, we calculate the overlaps of the main component $\Phi_{v_+}^F(I, R)$ of the FR with the field-free vibrational

TABLE I. Overlaps $S_v(I)$ of the box-normalized main adiabatic component of the FR with the field-free vibrational levels ($v = 16, 17, 18$) for different field intensities. The last column indicates the contrast defined as S_{18}/S_{17} .

I (GW/cm ²)	S_{18}	S_{17}	S_{16}	Contrast
1.0	0.876	0.407	9.3×10^{-2}	2.15
2.0	0.855	0.389	9.4×10^{-2}	2.20
3.04	0.818	0.333	8.7×10^{-2}	2.45
4.0	0.788	0.290	5.5×10^{-2}	2.72

wave functions $\chi_{gv}(R)$:

$$S_v(I) = \frac{|\langle \chi_{gv} | \Phi_{vk}^F(I, R) \rangle|}{\|\chi_{gv}\| \|\Phi_{v+}^F(I, R)\|}. \quad (18)$$

This calculation is conducted by extracting the real part of the main adiabatic component of $\Phi_{v+}^F(I, R)$ from a six-channel (NV = 6, NC = 1) model, as discussed previously, for some intensities including the ZWR one. The results are gathered in Table I.

Three observations are in order: (i) There are important differences between $v = 18, 17$, and 16 . In particular, the overlaps with $v = 16$ are negligible. In *a fortiori* way, the ones affecting $v < 16$ will be even less. We can thus focus on $v = 18$ and 17 for the main projection components of the long-range FR, with a large dominance on $v = 18$ (about 0.8 as compared to 0.3 on $v = 17$ for the ZWR intensity of 3.04 GW/cm²). (ii) The contrasts defined as the ratios of S_{18}/S_{17} , are regularly increasing with intensity. The passage from the ZWR intensity does unfortunately not give rise to any local enhancement that could be exploited in a filtrationlike strategy. (iii) However, referring to a control strategy with an adiabatically rising pulse, followed by a plateau at I_{ZWR} with a duration of about 80 ps, resonances originating from $v = 17$ and 16 will be completely washed out. Moreover, even a plateau duration of 0.4 ps would be enough to deplete the $v = 17$ resonance. The overlap with $v = 16$ (although still present for such pulse duration) being negligible, the population (probability density) trapped in the ZWR will finally be adiabatically transported in, but a single excited vibrational level ($v = 18$) of the ground-state potential, which precisely is the objective of our control scheme.

V. CONCLUSION AND PERSPECTIVES

In summary, on a *structural* basis, we have clearly evidenced the possibility to produce a quasistable molecular system (LBM) for which the interatomic binding forces are laser induced. In contrast with the standard field-free molecule where the interatomic binding forces are of chemical origin (CBM), the LBM system is described by long-range finite-lifetime Feshbach resonances that could be controlled, up to a ZWR formation. This leads to a stable molecule with different controllable structural properties than the CBM. From a *dynamical* viewpoint, we have also shown how this LBM once formed by an adiabatic switching of a laser pulse, will project preferentially on three of the most excited field-free vibrational levels ($v = 18, 17, 16$). Moreover, a filtration

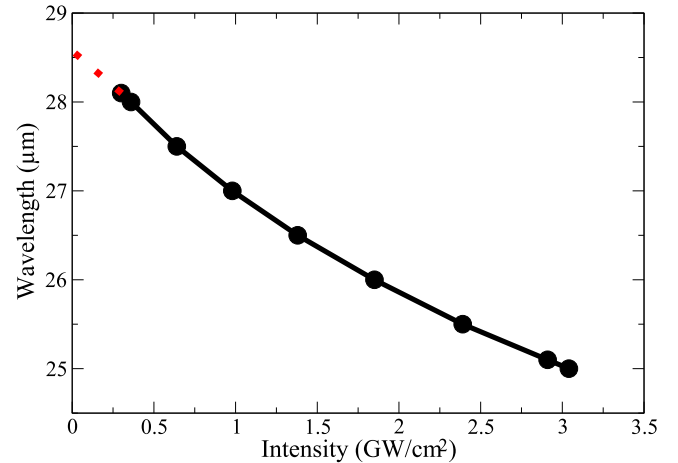


FIG. 20. ZWR loci in the laser parameter plane (wavelength versus intensity) The solid black dots correspond to couples (λ_{ZWR}, I_{ZWR}) producing a given ZWR. The solid line corresponds to an interpolation, and the red dots a plausible extrapolation, showing the possibility to obtain ZWRs even for very low intensities, provided that the wavelength is accurately chosen.

strategy is referred to for defining a pulse duration such as to dissociate all population deposited on vibrational excited states of the CBM, except $v = 18$. Generalizing ZWR to the multiphoton context and using it as a basic ingredient for two mechanisms, namely, trapping of the scattering wave packet and filtration among excited vibrational levels, we have worked out a full optical control strategy for a laser-assisted collision process ultimately leading to a single electronic and vibrational state of a stable molecule.

We emphasize that our study should be considered as a principle of concept. We claim that, both the choice of the molecular system itself and the laser characteristics present the potentiality to be further adjusted, to fit the requirements of a specific experimental situation. More precisely, concerning the molecule, H_2^+ is just an example of a homonuclear diatomic system. The low-dimension assumption, in relation with its field-induced alignment, could be removed by introducing rotational dynamics. We have previously shown that this would amount to additional channels in the Floquet description, but still compatible with the interference mechanism leading to a ZWR [42]. As for the role of the charge resonance enhanced transition dipole that has a major impact on the asymptotic region, where precisely the long-range FRs are localized, it has been analyzed in detail, uncovering thus all cases presenting such a challenging difficulty. Concerning the wavelength and intensity range of the laser parameters, we have proceeded to a specific choice based on a comprehensive argumentation. It is, however, important to note that other couples of (λ, I) are also possible. In particular, the destructive interference leading to the ZWR can be obtained even with much lower intensities, provided that the wavelength is carefully adjusted for the coincidence condition [Eqs. (14) and (15)] to be fulfilled. An example based on converged quantum calculations is given in Fig. 20. We have already proven the existence of such ZWRs occurring for low intensities (on an absolute scale) still giving rise to high nonlinearity, as they are

responsible of radiative couplings among energetically close enough vibrational levels resulting from a specific photon dressing [43]. In this work, we fix our choice on a more general presentation with a thorough discussion of multiphoton dynamics, more pedagogically illustrated with higher intensities and shorter wavelengths, while keeping some flexibility in their choice.

The future of this work will be a complete dynamical description of a laser-controlled collision process, based on the mechanisms which have been so far discussed. This should ultimately be conducted together with an optimization of the issue of connecting the initial collisional wave packet to the FR. As mentioned in the literature, this could be achieved referring to two strategies: (i) modeling the scattering using a Gaussian wave packet with a rather low group velocity, imposing an inward propagation to meet the FR with a favorable overlap (choice of sharp enough energy distribution, velocity, and initial spatial position); (ii) putting the whole system in a harmonic trap with large spatial extension, describing the relative motion between atoms, and using a laser field to

induce a dipole transition to associate the lowest trap level to the FR. More precisely, a pulse shape with a time-adiabatic coupling has to be worked out to connect the initial Gaussian wave packet to the FR which actually has merged in a ZWR, through a field intensity rising from $I = 0$ to I_{ZWR} . The adiabatic switching seems an advantage to progressively follow the ZWR, as displayed in Fig. 20 without any population loss and, more importantly, avoiding mathematical issues related with the morphology, in terms of exceptional points, of the non-Hermitian Hamiltonian [9]. The previously described filtration strategy will then prepare a single excited level $v = 18$, from which a standard STIRAP technique could bring the population on $v = 0$. This is ultimately an alternative way to prepare an ultracold molecule.

ACKNOWLEDGMENTS

O.A. acknowledges Prof. O. Dulieu, Prof. M. Desouter-Lecomte, Prof. E. Luc-Koenig, and Dr. A. Devolder for fruitful discussions.

-
- [1] K. E. Strecker, G. B. Partridge, and R. G. Hulet, *Phys. Rev. Lett.* **91**, 080406 (2003).
- [2] V. A. Yurovsky, A. Ben-Reuven, P. S. Julienne, and C. J. Williams, *Phys. Rev. A* **62**, 043605 (2000).
- [3] V. A. Yurovsky and A. Ben-Reuven, *Phys. Rev. A* **67**, 043611 (2003).
- [4] F. H. Mies, E. Tiesinga, and P. S. Julienne, *Phys. Rev. A* **61**, 022721 (2000).
- [5] S. Kotochigova, *Phys. Rev. Lett.* **99**, 073003 (2007).
- [6] F. A. van Abeelen and B. J. Verhaar, *Phys. Rev. Lett.* **83**, 1550 (1999).
- [7] O. Atabek, R. Lefebvre, A. Jaouadi, and M. Desouter-Lecomte, *Phys. Rev. A* **87**, 031403(R) (2013).
- [8] A. Leclerc, D. Viennot, G. Jolicard, R. Lefebvre, and O. Atabek, *Phys. Rev. A* **94**, 043409 (2016).
- [9] A. Leclerc, D. Viennot, G. Jolicard, R. Lefebvre, and O. Atabek, *J. Phys. B: At., Mol. Opt. Phys.* **50**, 234002 (2017).
- [10] A. Devolder, E. Luc-Koenig, O. Atabek, M. Desouter-Lecomte, and O. Dulieu, *Phys. Rev. A* **100**, 052703 (2019).
- [11] A. Devolder, E. Luc-Koenig, O. Atabek, M. Desouter-Lecomte, and O. Dulieu, *Phys. Rev. A* **98**, 053411 (2018).
- [12] A. Giusti-Suzor and F. H. Mies, *Phys. Rev. Lett.* **68**, 3869 (1992).
- [13] L. J. Frasinski, J. H. Posthumus, J. Plumridge, K. Codling, P. F. Taday, and A. J. Langley, *Phys. Rev. Lett.* **83**, 3625 (1999); L. J. Frasinski, J. Plumridge, J. H. Posthumus, K. Codling, P. F. Taday, E. J. Divall, and A. J. Langley, *ibid.* **86**, 2541 (2001).
- [14] A. D. Bandrauk, E. E. Aubanel, and J. M. Gauthier, in *Molecules in Laser Fields*, edited by A. D. Bandrauk (Marcel Dekker, New York, 1994), pp. 109–179.
- [15] K. Bergmann, N. V. Vitanov, and B. W. Shore, *J. Chem. Phys.* **142**, 170901 (2015).
- [16] S. Stellmer, B. Pasquiou, R. Grimm, and F. Schreck, *Phys. Rev. Lett.* **109**, 115302 (2012).
- [17] A. Ciamei, A. Bayerle, C.-C. Chen, B. Pasquiou, and F. Schreck, *Phys. Rev. A* **96**, 013406 (2017).
- [18] A. D. Bandrauk, E. Constant, and J. M. Gauthier, *J. Phys. (France) II* **1**, 1033 (1991).
- [19] T. Zuo and A. D. Bandrauk, *Phys. Rev. A* **52**, R2511(R) (1995).
- [20] A. D. Bandrauk and M. S. Child, *Mol. Phys.* **19**, 95 (1970).
- [21] M. S. Child, *Mol. Phys.* **32**, 1495 (1976).
- [22] F. H. Stillinger and D. R. Herrick, *Phys. Rev. A* **11**, 446 (1975).
- [23] H. Friedrich and D. Wintgen, *Phys. Rev. A* **32**, 3231 (1985).
- [24] O. Atabek, R. Lefebvre, and F. X. Gad ea, *Phys. Rev. A*, **74**, 063412 (2006).
- [25] O. Atabek, R. Lefebvre, and T. T. Nguyen-Dang, in *Handbook of Numerical Analysis*, Vol. X, edited by C. Le Bris (Elsevier, New York, 2003).
- [26] A. F. J. Siegert, *Phys. Rev.* **56**, 750 (1939).
- [27] W. P. Reinhardt, *Annu. Rev. Phys. Chem.* **33**, 223 (1982).
- [28] F. V. Bunkin, I. I. Tugov, and A. F. J. Siegert, *Phys. Rev. A* **8**, 601 (1973).
- [29] R. E. Moss, *Mol. Phys.* **78**, 371 (1993); **80**, 1541 (1993).
- [30] R. E. Moss, *J. Phys. B: At., Mol. Opt. Phys.* **32**, L89 (1993).
- [31] J. Carbonell, R. Lazauskas, D. Delande, L. Hilico, and S. Kılıç, *Europhys. Lett.* **64**, 316 (2003).
- [32] L. Fox, *The Numerical Solution of Two-Point Boundary Value Problems in Ordinary Differential Equations* (Oxford University Press, London, 1957).
- [33] D. W. Norcross and M. J. Seaton, *J. Phys. B: At. Mol. Phys.* **6**, 614 (1973).
- [34] M. S. Child, *Semiclassical Mechanics with Molecular Applications* (Clarendon, Oxford, 1991).
- [35] M. Chrysos, O. Atabek, and R. Lefebvre, *Phys. Rev. A* **48**, 3845 (1993).
- [36] M. Chrysos, O. Atabek, and R. Lefebvre, *Phys. Rev. A* **48**, 3855 (1993).
- [37] O. Atabek and R. Lefebvre, *Mol. Phys.* **117**, 2010 (2019).

- [38] A. Jaouadi, R. Lefebvre, and O. Atabek, *Phys. Rev. A* **95**, 063409 (2017).
- [39] J. M. Peek, *J. Chem. Phys.* **50**, 4595 (1969).
- [40] O. Atabek and R. Lefebvre, *Phys. Rev. A* **78**, 043419 (2008).
- [41] N. Moiseyev, *Phys. Rep.* **302**, 212 (1998); *Non Hermitian Quantum Mechanics* (Cambridge University Press, Cambridge, 2011); N. Moiseyev and U. Peskin, *Phys. Rev. A* **42**, 255 (1990).
- [42] O. Atabek, R. Lefebvre, C. Lefebvre, and T. T. Nguyen-Dang, *Phys. Rev. A* **77**, 043413 (2008).
- [43] R. Lefebvre and O. Atabek, *Int. J. Quantum Chem.* **109**, 3423 (2009).